Astron. Astrophys. 335, 134–144 (1998)

ASTRONOMY
AND
ASTROPHYSICS

Acceleration of ultra-high energy cosmic ray particles in relativistic jets in extragalactic radio sources

M. Ostrowski

Observatorium Astronomiczne, Uniwersytet Jagielloński, ul.Orla 171, PL-30-244 Kraków, Poland

Received 1 July 1997 / Accepted 2 March 1998

Abstract. A mechanism of ultra-high energy cosmic ray acceleration in extragalactic radio sources, at the interface between the *relativistic* jet and the surrounding medium, is discussed as a supplement to the shock acceleration in 'hot spots'. Due to crossing the tangential discontinuity of the velocity the particle can gain an amount of energy comparable to the energy gain at the shock crossing. However, the spectrum of particles accelerated at the jet side boundary is expected to be much flatter than the one formed at the shock. Due to this fact, particles accelerated at the boundary can dominate the overall spectrum at highest energies. In conditions characteristic to extragalactic jets' terminal shocks, the mechanism naturally provides the particles with $E \sim 10^{20}$ eV and complies with the efficiency requirements. The spectrum formation near the cut-off energy due to action of both the shock acceleration and the tangential discontinuity acceleration is modelled with the Monte Carlo particle simulations. It confirms that the upper energy limit can surpass the shock acceleration estimate.

Key words: galaxies: jets – cosmic rays – acceleration of particles – shock waves

1. Introduction

Jet-like outflows are observed in a number of astrophysical environments, starting from young stars embedded in their parent molecular clouds, up to active extragalactic objects. In the later case, a number of interesting observational phenomena are noted over orders of magnitude of linear sizes. In particular, at the smallest milli-arc-second scales, one often observes relativistic jet velocities, with flow Lorentz factors γ_u reaching the values above 10 (cf. Ghisellini et al. 1996). At larger scales, velocity measurements are more difficult, but without entrainment of large amount of matter near the active galactic nuclear source the jet flow velocity must be also relativistic. A possible loading of a jet with matter is expected to be appended by a substantial amount of turbulence (Henriksen 1987) and related jet kinetic energy dissipation. However, in the FR II radio sources, there are often observed jets efficiently transporting energy to the far-away hot spots and any jet breaking mechanism cannot act too effectively near the central core. Also, the existing hydrodynamical simulations of relativistic jets show for possibility of extended stable jet structures (Marti et al. 1995, 1997; Gómez et al. 1995). Another argument suggesting the relativistic jet speed at all scales, may be based on the visible asymmetry of jets with respect to the nuclear source, if one believes the effect is caused by the high velocity of the essentially bi-symmetric outflow (cf. Bridle et al. 1994). Let us also note that the Meisenheimer et al. (1989) modelling of the shock acceleration process at extragalactic radio-source hot spots yields 'the best-guess' jet velocities in the range $(0.1, 0.6)$

The relativistic movement of the jet leads to shock wave formation in places where an obstacle or perturbation of the flow creates a sudden velocity jump. For jets loaded with a cold plasma the highly oblique conical shocks are formed within the jet tube. These shocks can have a non-relativistic character, involving the velocity jump perpendicular to the shock surface much smaller than the overall jet velocity $U \sim c$. They lead to a limited kinetic energy dissipation and are usually claimed to be responsible for forming the so called 'knots' along the jet. A much more powerful shock is formed at the final working surface of the jet. There, a substantial fraction of the jet energy is transferred into heating the jet's plasma, generating strong turbulence, boosting magnetic fields within the turbulent volume, and finally accelerating electrons and nuclei to cosmic ray energies. Rachen & Biermann (1993) considered the process of particle acceleration to ultra-high energies (UHE) at such shocks. They show that given the favourable conditions the UHE particles up to $\sim 10^{20}$ eV can be formed. Then Rachen et al. (1993) show that assumption of UHE particle acceleration in extragalactic powerful radio sources is compatible with the current measurements of cosmic ray abundances and spectra at energies above 10^{17} eV. Additionally, the arrival directions of cosmic ray particles observed above 10 EeV are correlated with the local galactic supercluster structure (Stanev et al. 1995; see, also, Medina Tanco et al. 1996, Sigl 1996, Sigl et al. 1995, 1997, Hayashida et al. 1996, Elbert & Sommers 1995, Geddes et al. 1996 and Medina Tanco 1998). An alternative model involving the several-Mpc-scale non-relativistic shocks in galaxy clusters is proposed by Kang et al. (1996; see also Kang et al. 1997).

As noted by us (Ostrowski 1990; henceforth Paper I) a tangential discontinuity of the velocity field can also provide an

Send offprint requests to: M. Ostrowski (mio@oa.uj.edu.pl)

efficient cosmic ray acceleration site if the considered velocity difference U is relativistic and the sufficient amount of turbulence on both its' sides is present. The problem was extensively discussed in the early eighties by Berezhko with collaborators (see the review by Berezhko 1990) and in the diffusive limit by Earl et al. (1988) and Jokipii et al. (1989). In the present paper we consider the process of ultra high energy cosmic ray acceleration in relativistic jets including the possibility of such boundary layer acceleration. As the considerations of Rachen & Biermann (1993) treat the acceleration process at relativistic shock in a somewhat simplified way (see, also Sigl et al. 1995), in the first part of the next section (Sect. 2.1) we review this process in some detail in order to understand the interrelations between the conditions existing near the shock, the accelerated particle spectrum and the particle's upper energy limit. Then, in Sect. 2.2, we present a short description of the basic physical model for the considered acceleration process acting at the jet boundary. We show (Sect. 2.3) that in the conditions characteristic for relativistic jets in extragalactic radio sources, particles with energies above 10^{20} eV can be produced in this process without extreme parameter fitting. The required efficiency is discussed in Sect. 2.4. We confirm the estimates presented previously for the shock acceleration, showing that the UHE particle flux observed at the Earth can be reproduced as a result of acceleration processes in jets of nearby powerful radio sources. In Sect. 3 we discuss the problem of the particles' spectrum. With the use of Monte Carlo simulations, we consider the action of both processes acting near the terminal shock in a relativistic jet. Modification of the spectrum due to varying boundary conditions and jet velocity is discussed for the case of (e^-, p) jets expected to occur in the powerful FRII radio sources (cf. Celotti & Fabian 1993). The derived particle's upper energy limits are above the shock acceleration estimates and the spectrum modification at highest energies can resemble the observed above 10 EeV 'ankle' structure. A short summary and final remarks are presented in Sect. 4. A preliminary report about this work was presented in Ostrowski (1993b, 1996).

For the discussion that follows, we consider the jet propagating with the relativistic velocity, $U \sim c$. We use c = 1 units.

2. Acceleration processes in relativistic jets

The present considerations attempt to extend the discussion of particle acceleration at shock waves formed in the end points of jets by including an additional acceleration process acting at the jet boundary layer. For particles with UHE energies both the shock transition as well as the velocity transition layer between the jet and the surrounding medium ('cocoon') can be approximated as surfaces of discontinuous velocity change[1]. Basing on such approximation we compare the acceleration at the non-compressive tangential discontinuity at the jet side boundary and the compressive terminal shock discontinuity.

[1] One may also note that in the perfect fluid simulations of relativistic jets by Marti et al. (1995, 1997) the numerical viscosity inherent to such approach does not lead to generation of an extended shear layer.

2.1. Shock acceleration in a hot spot

A review of the problems related to energetic particle acceleration at relativistic shock waves is presented by Ostrowski (1996) and Kirk (1997). In the present section we summarize some most important findings in this subject. The main difficulty in considering cosmic ray acceleration at relativistic shocks arises from the substantial particle anisotropies involved. A consistent approach to the first order Fermi acceleration at such a shock propagating along the background magnetic field ('parallel shock') was conceived by Kirk & Schneider (1987) who obtained solutions to a kinetic equation of the Fokker–Planck type with a pitch-angle diffusion scattering term. More general conditions at the parallel shock were considered by Heavens & Drury (1988), who took into consideration the fluid dynamics of relativistic shock waves. For a shock propagating in the cold (e, p) plasma a trend was revealed to make the accelerated particle spectrum slightly flatter ($\sigma \approx 3.7$) for the shock velocity, U, growing up to roughly $0.5c$, and, then, increasing the inclination with further growth of U up to $\sigma \approx 4.2$ at the highest considered velocity $u = 0.98$. However, the resulting varying spectral index could still be reasonably approximated with the non-relativistic expression $\sigma = 3R/(R-1)$, where R is the shock compression ratio. They also noted that the spectrum inclination depends on the perturbations' spectrum near the shock, in contrast to the non-relativistic case. A qualitatively new possibility was revealed by Kirk & Heavens (1989) who considered the acceleration process in shocks with magnetic fields oblique to the shock normal (see also Ballard & Heavens 1991 and Ostrowski 1991). They demonstrated, again in contrast to the non-relativistic results, that such shocks led to flatter spectra than do the parallel ones, with $\sigma \approx 3.0$ for the (subluminal) quasi-perpendicular shocks. Their work relied on the assumption of adiabatic invariant $p_\perp^2/B$ conservation for particles interacting with the shock and, thus, was limited to only slightly perturbed background magnetic fields. A different approach to particle acceleration was presented by Begelman & Kirk (1990), who noted that in relativistic shocks most field configurations lead to super-luminal conditions. Then particles can be energized in a single shock transmission only, accompanied with a limited energy gain, but the acceleration in relativistic conditions is more efficient than that predicted by a simple adiabatic theory. The acceleration process in the presence of finite amplitude perturbations of the magnetic field was considered by Ostrowski (1991; 1993a), Ballard & Heavens (1992) and Bednarz & Ostrowski (1996). The considerations involved the Monte Carlo particle simulations for shocks with oblique perturbed magnetic fields. It was noted that the spectral index was not a monotonic function of the perturbation amplitude, enabling for the steeper spectra at intermediate perturbation amplitudes than those for the limits of small and large amplitudes. It has also been revealed that the conditions leading to very flat spectra involve an energetic particle density jump at the shock and probably lead to instability. The acceleration process in the case of a perpendicular shock shows a transition between the compressive acceleration described by Begelman & Kirk (1990)

and, at larger perturbations, the regime allowing for formation of a wide range power-law spectrum. As a conclusion of this short review one should note that the present theory is unable to predict the spectral index of particles accelerated at the relativistic shock wave, e.g., the possible range of indices arising in computations for the sub-luminal shocks propagating in the cold (e, p) plasma is $3.0 < \sigma < 4.5$.

To date, there was somewhat superficial information on the acceleration time scales, T_{acc}, in relativistic shocks as the applied approaches often neglected or underestimated a significant factor controlling the acceleration process – the particle anisotropy. The realistic particle distributions are considered in Bednarz & Ostrowski (1996; see also Ellison et al. 1990 and Naito & Takahara 1995 for specific cases) who considered shocks with oblique, sub- and super-luminal magnetic field configurations and with finite amplitude perturbations, δB. At parallel shocks, T_{acc} diminishes with increasing perturbation amplitude and the shock velocity U_1. A new feature discovered in oblique shocks is that due to the cross-field diffusion T_{acc} can change with δB in a non-monotonic way. The acceleration process at the super-luminal shock leading to the power-law spectrum is possible only in the presence of a large amplitude turbulence. Then, in contrast to the quasi-parallel shocks, T_{acc} increases with the increasing wave amplitude. For *mildly* relativistic shocks, in some magnetic field configurations one discovers a possibility to have extremely short acceleration time scales, comparable, or even smaller than the particle gyroperiod in the magnetic field upstream of the shock. It is also noted that there exist a coupling between the acceleration time scale and the resulting particle spectral index. Again, the above variety of different results illustrates the difficulty in providing an accurate acceleration time scale estimate without a detailed knowledge of the conditions in the shock.

A discussion of UHE particle acceleration at mildly relativistic shocks formed at the powerful radio source hot spots was presented by Rachen & Bierman (1993) and Sigl et al. (1995). The partly qualitative considerations show a potential difficulty in accelerating particles to the highest required energies. Besides the difficulties with the acceleration time scale there are even more severe constraints for the particle energy due to the boundary conditions: the finite perpendicular extent of the jet and the finite extent of the shock's downstream region situated within the radio source hot spot. The considerations of the time dependent acceleration at shocks described above (Bednarz & Ostrowski 1996) allow for a very rapid acceleration only in some particular conditions. One should also be aware of the another problem. As discussed above, due to an anisotropic particle distribution at the shock, the different physical factors acting near it can substantially modify the particle energy distribution. Thus, let us stress again, the theory is not able to predict every particular spectral index for the accelerated particles (cf. Ostrowski 1994, 1996) or any particular acceleration time scale and any attempt to compare such existing predictions to the observations bears a substantial degree of arbitrariness.

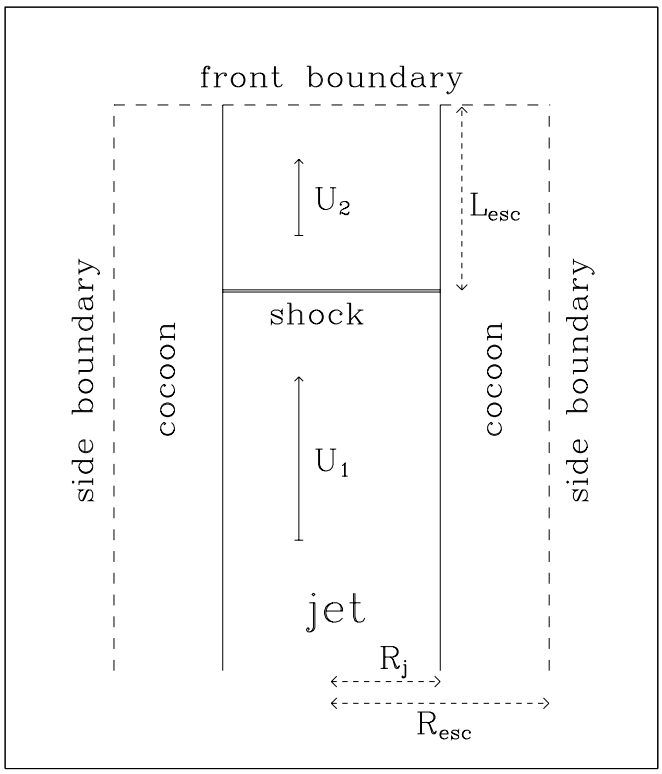

Fig. 1. A schematic representation of the terminal shock neighbourhood. The velocities and distances used in the text are indicated.

2.2. Acceleration process at the jet side boundary

A tangential discontinuity of the velocity field (or a shear layer) occurring at the jet side boundary can be an efficient cosmic ray acceleration site if the considered velocity difference, U, is relativistic and the sufficient amount of turbulence on its both sides is present [2] (Paper I, Ostrowski 1997). If near the jet boundary particles exist with gyroradii (or mean free paths normal to the boundary) comparable to the actual thickness of the shear-layer interface, the acceleration process can be very rapid. One may note, that the particles with energies > 1 EeV, of interest here, could satisfy the last condition naturally. Any high energy particle crossing the boundary from, say, region I (within the jet) to region II (off the jet), changes its energy, E, according to the respective Lorentz transformation. It can gain or loose energy. In the case of a uniform magnetic field in region II, the successive transformation at the next boundary crossing, II $\rightarrow$ I, changes the particle energy back to the original value. However, in the presence of perturbations acting at particle orbits between the successive boundary crossings there is a positive mean energy change:

$$< \Delta E > \; = \rho_E \, (\gamma_u - 1) \, E \qquad , \qquad (1)$$

where $\gamma_u \equiv (1 - U^2)^{-1/2}$ is the flow Lorentz factor. The numerical factor ρ_E depends on particle anisotropy at discontinuity.

[2] For simplicity, we consider the magnetic field perturbations static in the local plasma rest frame and thus we neglect any additional acceleration due to the second-order Fermi process.

It increases with the growing field perturbations' amplitude but slowly decreases with growing flow velocity. Particle simulations described in Paper I give values for ρ_E within the strong scattering limit as a substantial fraction of unity. During the acceleration process, particle scattering is accompanied by the jet's momentum transfer into the medium surrounding it. On average, a single particle with momentum p transports the following amount of momentum across the jet's boundary:

$$< \Delta p > = < \Delta p_z > = \rho_p \, U \, p \qquad , \qquad (2)$$

where the value of p is given as the one after transmission and the z-axis of the reference frame is chosen along the flow velocity. The numerical factor ρ_p depends on the scattering conditions near the discontinuity and it can reach values also being a substantial fraction of unity. As a result, there exists a drag force *per unit surface* of the jet boundary acting on the medium along the jet, of a magnitude order same as the accelerated particles' energy density. Independent of the exact value of ρ_E, the acceleration process can proceed very fast in the case of the mean magnetic field being parallel to the boundary (cf. Coleman & Bicknell 1988, Fedorenko & Courvoisier 1996) because particles can be removed at a distance from the accelerating interface only in the inefficient process of cross-field diffusion. One may note that in the case of a non-relativistic velocity jump, $U \ll c$, the acceleration process becomes of the second-order in U/c and a rather slow one.

2.3. The upper energy limit for the tangential discontinuity acceleration

For acceleration at the considered tangential discontinuity the acceleration time scale T_{acc} – as long as the flow is mildly relativistic – can be approximately determined by the mean time between boundary crossings, $< \Delta t >$, and the mean energy gain at the crossing, $< \Delta E >$ (Eq. 1; cf. Bednarz & Ostrowski (1996) for the case of non-vanishing correlations between Δt and ΔE, when $\Delta E \sim E$). Within a simple diffusive model in Paper I, the time T_{acc} is expressed with the use of λ/c, where λ is the particle mean free path. T_{acc} depends on a number of physical factors, including jet velocity and magnetic field structure determining parameters of particle wandering at the acceleration region and the mean energy gain at individual boundary crossing. Thus we express the acceleration time scale as

$$T_{acc} = \alpha \, \lambda \, / \, c \qquad , \qquad (3)$$

where α is a numerical factor depending on the local conditions at, and near the jet, including the escape boundary distance, the turbulent magnetic field structure near the flow discontinuity and the flow velocity. For the strong scattering limit the estimates of Paper I give the values of α between, say, 10 and 1, if we require the spectrum to be sufficiently flat, within the velocity range $(0.5,\ 0.99)$ [3]. The actual conditions are different

[3] One should note that the time scales given in Paper I are derived for stationary spectra. Thus, it provides only the upper limits for the

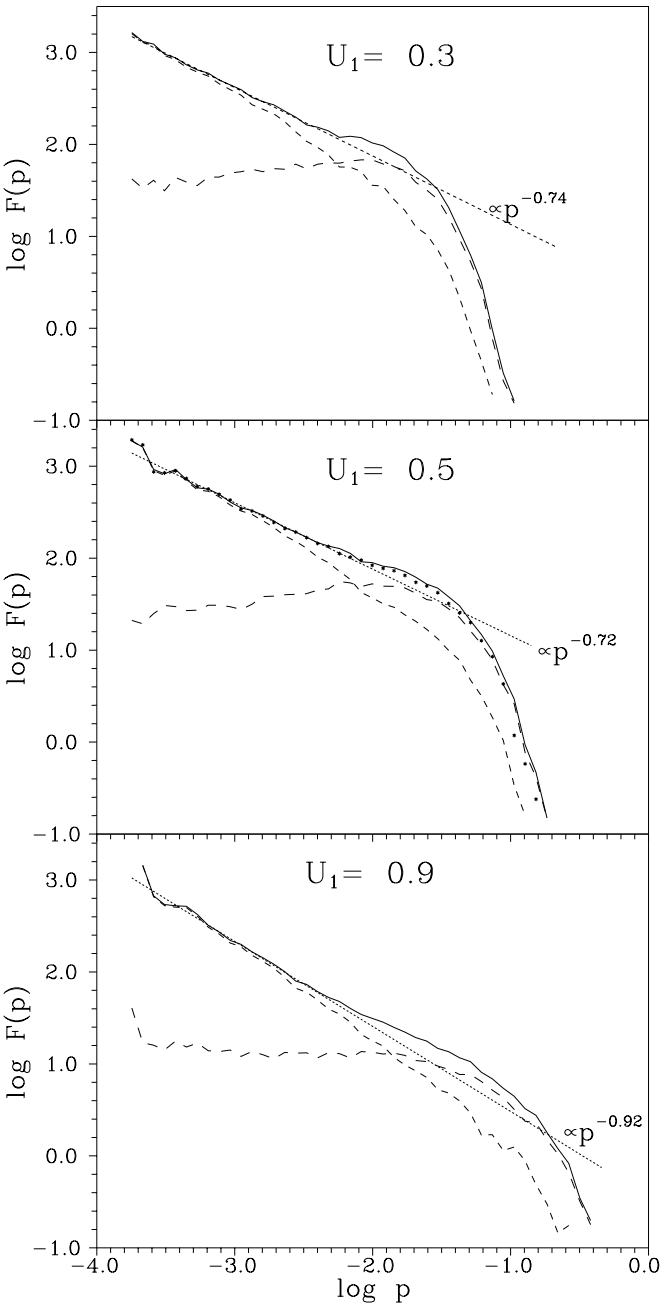

Fig. 2. Particle spectra derived for the acceleration process involving the first-order Fermi acceleration at the jet terminal shock and the acceleration at the jet-cocoon interface. The case with $D = 0.97$ and a seed particle injection at the shock is considered. The spectrum of all escaping particles is presented with a full line, while with dashed lines the spectra at the respective escape boundaries: medium dashes for the front boundary and long dashes for the side boundary. We consider the case with the front boundary placed $L_{esc} = R_j$ downstream of the shock and the side boundary in the distance $R_{esc} = 2R_j$ from the jet axis. For the low energy part of the front boundary spectrum we provide a power–law fit representing the 'pure' shock spectrum without the cut-off (short dashes). At the successive panels we present the cases for $U_1 = 0.3$, 0.5 and 0.9 . For comparison, the spectrum formed at the shock with neglected energy changes at the jet side boundary is presented for the case of $U_1 = 0.5$ (individual points).

from the plane-parallel case considered in Paper I, but we expect the above estimates to be still valid, as long as the particle gyroradius $r_g(E)$ is smaller than the jet radius R_j. If the perturbations are due to growing instabilities near the jet boundary, one may expect them to reach substantial amplitudes up to and above the kiloparsec scales that are of interest here, leading to magnetic field perturbations [4] $\delta B/B \sim 1$ and $\lambda \sim r_g$. Then, the acceleration time scale becomes

$$T_{acc} = 0.1\,\alpha\,\gamma_p\,B_m^{-1} \quad [s] \qquad . \qquad (4)$$

For numerical evaluations, let us consider the radio source jet on the $\sim 10^{2-3}$ kpc scale of interest here. To estimate the upper energy limit for accelerated particles, at first one should compare the time scale for energy losses due to radiation and inelastic collisions to the acceleration time scale. The discussion of possible loss processes is presented by Rachen & Biermann (1993), who provide the loss time scale for protons as

$$T_{loss} \simeq 5 \cdot 10^{24}\,B_m^{-2}\,(1+Xa)^{-1}\,\gamma_p^{-1} \quad [s] \qquad (5)$$

where B_m is the magnetic field in mGs units, a is the ratio of the energy density of the ambient photon field relative to that of the magnetic field, X is a quantity for the relative strength of $p\gamma$ interactions compared to synchrotron radiation and γ_p is the proton Lorentz factor. For cosmic ray protons the acceleration dominates over the losses (Eq-s 4,5) up to the maximum energy

$$\gamma_{p,max} \sim 10^{13}\,[\alpha\,B_m(1+Xa)]^{-1/2} \qquad . \qquad (6)$$

This equation can easily yield a large limiting $\gamma_{p,max} \sim 10^{13}$ with moderate jet parameters (e.g. with $\alpha \approx 10$, $B_m \approx 0.1$ and $Xa << 1$). However, one should note that the particle gyroradius $r_g(\gamma_p)$ provides the minimum for the acceleration region's spatial extent allowing particles to reach the predicted value of γ_p. Thus, for the actual particle maximum energy $\gamma^*_{p,max}$ the jet radius should be larger than the respective gyroradius $r_g(\gamma^*_{p,max})$ (cf. simulations presented in Sect. 3). From the observations of 6 objects Meisenhaimer et al. (1989) derived the following 'best-guess' parameters for the hot spots with emission extending up to the infrared or optical wavelengths: $B_m \sim (0.2 - 0.8)$ mGs, hot spot diameters $D \sim (0.7 - 5.0)$ kpc, jet velocities within $(0.1, 0.6)$ c and the shock compression ratios in the range $(3.5, 4.8)$. If, with a bit of optimism, one deduces from these estimates the jet (i.e. upstream the shock) parameters $B_j \sim 0.2$ mGs, $R_j \sim D \sim 2$ kpc the maximum particle energy can reach 10^{20} eV ($\gamma_p \sim 10^{10}$). This value is substantially smaller than the upper limit given in Eq. 6 and scales like $R_j/(2\,\mathrm{kpc}) \times B_j/(2\,\mathrm{mGs})$.

2.4. The required efficiency

Let us consider an isotropic power-law phase-space cosmic ray distribution with a cut-off at the momentum p_{max}: $f(p) = C\,p^{-\sigma}\,H(p_{max}-p)$, where H is the Heaviside step function and σ is the spectral index. For a flat spectrum, $\sigma < 4.0$, the cosmic ray energy density ($\propto \frac{1}{4-\sigma}\,p_{max}^{4-\sigma}$) peaks near the cut-off. For example, for $\sigma = 3.0$, 99% of the cosmic ray energy density falls at the last two energy decades. For powerful sources, the rate of energy extraction from the galactic nucleus in a form of jet kinetic energy is estimated at $\sim 10^{59}$ eV/s. If a fraction η of this energy is transformed into UHE cosmic rays and the particles are transmitted spherically-symmetric around the source, then the flux at Earth reaches the value $\sim \eta\,10^7 D_{10}^{-2}$ eV/s/cm^2, where D_{10} is the source distance in units of 10 Mpc. Above we neglect losses between the particle source and the Earth. As the measurements in the range above 1 EeV give the energy flux $\sim 10^4$ eV/cm^2/s, it is enough to assume a small value $\eta \sim 10^{-3}$ to explain the observations with a single nearby source, or the respectively smaller value for numerous sources. For somewhat steeper spectra with $\sigma \approx 4.0$, the required particle production efficiency can be an order of magnitude larger. The analogous efficiency estimates are obtained by Rachen & Biermann (1993; see also Rachen et al. (1993) and further references listed in the first section) and for an alternative model, by Kang et al. (1997).

3. The accelerated particle spectrum

Below, with the use of the Monte Carlo simulations, we discuss the spectrum of particles accelerated at the jet if the acceleration process at the jet side-boundary is present. Let us note that in ultrarelativistic flows both processes - the acceleration at the terminal shock and at the considered here tangential discontinuity at the jet boundary - are in some way comparable. The mean relative energy gain of a particle at individual interaction with the relativistic shock, $< \Delta E/E >_{sh} \sim \gamma - 1$, where the Lorentz factor $\gamma \equiv (1-U^2)^{-1/2}$ and $U = (U_1 - U_2)/(1 - U_1 U_2) \sim 1$. An analogous estimate for the boundary acceleration (cf. Eq. 1) $< \Delta E/E >_{tang} \sim \gamma_1 - 1$ yields a somewhat larger energy gain, but for mildly relativistic flows the ratio $(\gamma - 1)/(\gamma_1 - 1) < 1$ is quite close to 1. Therefore the resulting acceleration depends roughly on the number of particle interactions with the shock and the boundary discontinuity, respectively. These numbers depend on numerous factors including the injection site of cosmic ray particles and the transport properties for these particles. For smaller velocities with $\gamma_1 \approx 1$ the shock acceleration becomes the first order process with $\Delta E/E \sim U$ and is expected to dominate over the second order tangential discontinuity acceleration (cf. Sect. 2.2).

As discussed in Sect. 2.1, the spectra of particles accelerated at relativistic shock waves depend in a large extent on the detailed conditions (magnetic field configuration, amplitude of field perturbations, etc.) near the shock. Unfortunately, these

actual process, where, at first, the accelerated particles appear at the discontinuity and they fill the full diffusive volume near the jet in the later times. This filling process is accompanied with the gradual flattening of the spectrum. If one inquires about the highest particle energies expected to occur at the discontinuity, a value of α close to 1 should be assumed in Eq. 3. Then, in the energy range close to the upper cut-off, the particle spectrum will be steeper than the stationary one (cf. also Ostrowski & Schlickeiser 1996).

[4] An alternative, outside the test particle approach, is provided by the anisotropic particle distribution near the boundary, inducing the resonance waves' due to streaming instability.

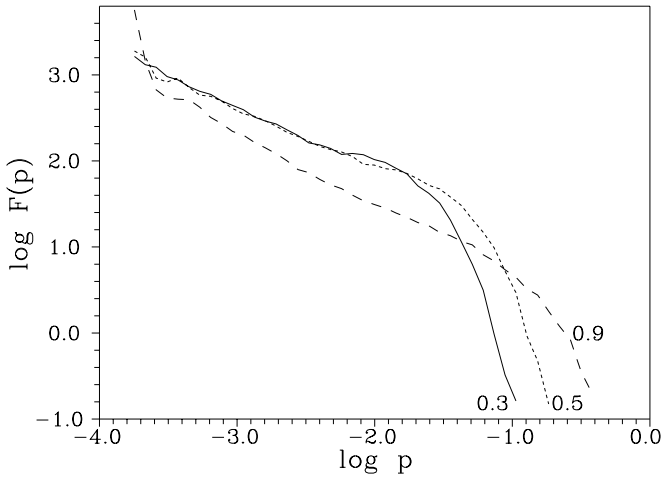

Fig. 3. Comparison of the total spectra from Fig. 2 for different flow velocities. The velocities are given near the respective curves.

conditions are usually poorly known and any consideration of the process must be based on several rough assumptions. Therefore, in the present simulations we do not attempt to reproduce a detailed shape of the particle spectrum in any definite astrophysical object, but, rather, we consider the form of spectrum modifications introduced to the standard *power-law with a cut-off* shock spectrum by additional acceleration at the jet boundary. In order to limit the number of free parameters we decided to model stationary particle spectra *without* taking the radiative losses into account, i.e. the upper energy limit of accelerated particles (cf. Rachen & Biermann 1993, Sigl et al. 1995) is fixed by the boundary conditions allowing for the escape of the highest energy particles. Below, we consider the simplest parallel shock configuration. One should note, however, that the derivations of the acceleration time scales in relativistic shocks by Naito & Takahara (1995) and Bednarz & Ostrowski (1996) suggest the possibility of more rapid acceleration in shocks with oblique magnetic fields. The situation with losses being important is commented in Sect. 4.

3.1. Monte Carlo modelling

In the simulations, we simplify the jet structure near the terminal shock as depicted in Fig. 1. The shock is in rest with respect to the cocoon surrounding the jet. The upstream plasma hitting the shock moves with the relativistic velocity U_1 and is advected downstream with the velocity, U_2. In present simulations we consider three values for the flow velocity, $U_1 = 0.3$, 0.5 and 0.9 of the light velocity. The shock compression ratio $R \equiv U_1/U_2$ is derived with the use of approximate formulae presented by Heavens & Drury (1988) for shock propagating in cold electron–proton plasma and a negligible dynamical role of the magnetic field. The analysis of Celotti & Fabian (1993) suggests that (e, p) plasma can be a viable jet content in the strong FRII radio sources. The conditions occurring behind the jet terminal shock due to the flow divergence are modelled by imposing the particle free escape boundary a finite distance, L_{esc}, downstream of the shock and in the adjoining front side of the cocoon ('a front boundary', cf. Fig. 1). We use the jet radius, R_j, as the unit to measure L_{esc} and other spatial distances. However, one should note that the physical barrier 'opposing' particle escape is defined by the downstream diffusive scale $L_{diff} \equiv \kappa_2/U_2$, where κ_2 is the downstream diffusion coefficient along the shock normal. Here the magnetic field is oriented along this normal and $\kappa_2 \equiv \kappa_{\parallel,2}$. The value of L_{esc} in units of L_{diff} scales as $p^{-1}\,D^{1/2}$, where $D \equiv \kappa_\perp/\kappa_\parallel$ and $\kappa_\parallel$ ($\kappa_\perp$) is the particle diffusion coefficient along (across) the magnetic field. Since the finite extent of the actual cocoon and all realistic magnetic field structures therein allow for particle escape to the sides we introduce another, tube–like free escape boundary surrounding the jet ('a side boundary') in a distance of R_{esc} from the jet axis. The unit for the particle momentum is defined by the 'effective' (cf. Bednarz & Ostrowski 1996) magnetic field, B_e, in such a way, that a particle with the momentum $p^* = 1.0$ has a gyroradius equal to the jet radius, $r_g^* = p^* c/(eB_e) = R_j$. A concept of the effective field is introduced to represent the additional magnetic field power contained in waves perturbing particle trajectories. The action of the effective field is observed in the simulations as bending of the particle trajectory at scales smaller than its gyroradius in the uniform component of the magnetic field, B_0. With a simplified scattering model applied, B_e is not uniquely defined (one is unable to evaluate the amount of turbulence at scales smaller than $\sim c\,\Delta t$), in the present simulations we use the value estimated by Bednarz & Ostrowski (1996) as $B_e = B_0\sqrt{1 + 4/9\,(\Delta\Omega/\Delta t)^2}$, where $\Delta\Omega$ is the maximum angular momentum scattering amplitude and Δt is the mean scattering time multiplied by the angular gyration velocity (here $= 1$). In the present simulations, the values $B_e = 32.0$ and 1.05 arise for $D = 0.97$ and 0.0013, the strong and the weak scattering cases, respectively.

Below, we consider spectra of particles escaping through the considered boundaries for the mono-energetic ($p_0 = 10^{-3}$ or $1.8\,10^{-4}$) seed particle injection either at the shock ($z_{inj} = 0$) or at the jet side boundary far upstream of the shock ($z_{inj} = -10^3 R_j$), and for different distances (L_{esc}, R_{esc}) of the boundaries. The particle distribution $F(p) \equiv d\,N(p)\,/\,d(\log p)$ [5], which gives the particle number per logarithmic momentum bandwidth, is derived for particles escaping through the boundaries. For simplicity, in order to limit the number of free parameters in the simulations, we assume the mean magnetic field to be parallel to the jet velocity both within the jet and in the cocoon (cf. Coleman & Bicknell 1988, Fedorenko &

ourvoisier 1996). In the examples presented below we consider a (resulting from simulations) ratio $D \equiv \kappa_\perp/\kappa_\parallel$ to be either 0.0013 (*small*) or 0.97 (*large* cross field diffusion). We consider these values as the effective ones, representing the transport properties of the medium with realistic magnetic field structures. The geometric pattern of the introduced particle trajectory perturbations' is taken to be the same at all momenta (Ostrowski 1991). Thus both diffusion coefficients are propor-

[5] For the power-law distribution the spectral index for $F(p)$ is $\sigma - 3$ (cf. Sect. 2.4).

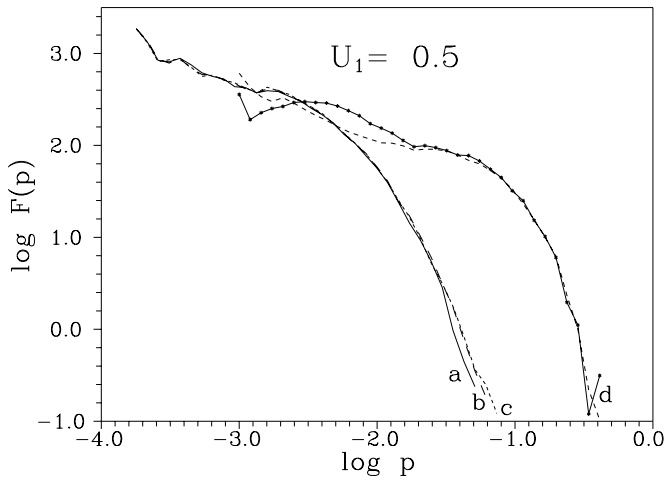

Fig. 4. Comparison of particle spectra for different distances to the jet side boundary for $U_1 = 0.5$. The case with $D = 0.97$ and the seed particle injection at the shock is considered. Three spectra are presented for $L_{esc} = 1.0$: a.) $R_{esc} = 1.1$, b.) $R_{esc} = 2.0$, c.) $R_{esc} = 11.0$, and two additional spectra for $R_{esc} = 11.0$: d.) $L_{esc} = 10.0$ and e.) $L_{esc} = 100.0$.

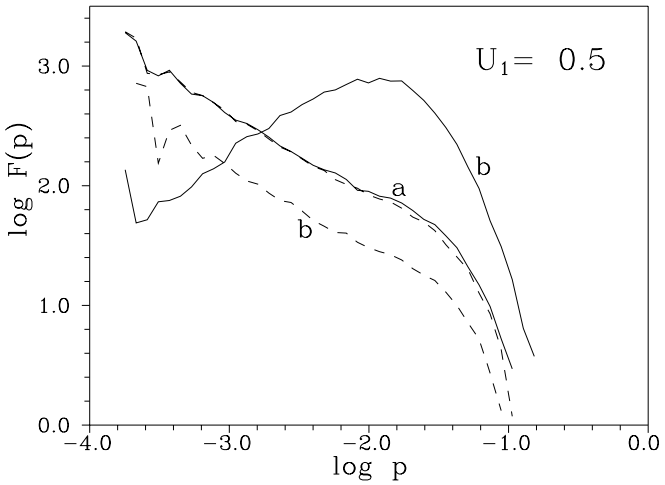

Fig. 5. The particle spectra formed with and without the jet boundary acceleration for $D = 0.97$. Spectra formed due to acceleration both at the jet boundary and at the terminal shock are presented with full lines, while the spectra for the neglected boundary acceleration are given with dashed lines. The results are presented for $R_{esc} = 2.0$, $L_{esc} = 1.0$ and a.) $z_{inj} = 0.0$ or b.) $z_{inj} = -1000.0$.

tional to the particle momentum and the above ratio of diffusion coefficients is constant. Further details of the simulations are described in Appendix A.

At Fig-s 2-4, we consider particle spectra for the seed particle injection at the shock. The fixed spatial distances to the escape boundaries are assumed, but the size of particle trajectory defined by its gyroradius, as well as the spatial diffusion coefficients, increase in proportion to the particle momentum. As a result, the escape probability grows with particle energy providing a cut-off in the spectrum. The energy scale of the cut-off is different for the front boundary spectrum and the side boundary spectrum, with the latter being often larger in our simulations. This difference can occur also in the case of numerical experiments with the jet boundary acceleration turned off. It is due to the fact that particles accelerated at the shock close to the jet boundary have the opportunity to diffuse back upstream across the static cocoon medium, to be accelerated again at the shock and then escape through the side boundary. The difference between these two scales increases for example, with the jet velocity, the extent of the diffusive cocoon, shifting the particle injection site upstream of the shock, increasing the effective particle radial diffusion coefficient. However, one should note that the role of the jet boundary acceleration is limited for the seed particle injection at the shock in the presence of the nearby front escape boundary (cf. Fig. 2, middle panel). As explained below the situation will change drastically for the injection at the jet boundary far upstream of the shock.

In the spectra presented at Fig. 2 three parts can be clearly separated. The first one, with a wavy behaviour, reflects the initial conditions of the mono-energetic injected spectrum interacting with the accelerating surfaces – for the shock injection only the shock acceleration is important in this range. In the remaining part of the spectrum, at energies directly preceding the cut-off energy, the spectrum exhibits some flattening with respect to the inclination of the lower energy part. The low energy section of the spectrum – within computational accuracy – coincides with the analytically derived inclination of the spectrum formed at the infinitely extended shock (cf. Heavens & Drury 1988). The spectrum flattening at larger energies occurs due to additional particle transport from the shock's downstream region to the upstream one through the cocoon surrounding the jet (this effect occurs also if there is no side boundary acceleration !), and inclusion of a very flat spectral component resulting from the side boundary acceleration (see below).

A comparison of particle spectra generated at jets with different velocities is presented in Fig. 3. One may note a systematic shift of the spectrum cut-off toward higher energies with an increase of the jet velocity. Additionally, at the low energy portion of the spectrum, the expected spectral index change can be observed. The influence of varying distances (L_{esc}, R_{esc}) at particle spectra can be evaluated by inspecting Fig. 4. Decreasing any boundary distance leads to decreasing the cut-off energy, however the actual changes depend in a substantial degree on the leading escape process removing particles from the acceleration region - either the diffusive/free-escape through the front boundary or the radial diffusion toward the side boundary. Let us finally stress, that even for an infinite diffusive volume surrounding the jet, the acceleration efficiency will decrease for particles with momenta $p > p^*$. Therefore, the upper momentum cut-off cannot reach values above the scale $\sim \gamma_u p^*$.

In Fig. 5 we compare spectra of particles injected at the jet side boundary far upstream of the shock, in the distance $10^3\, R_j$, to the spectra of particles injected at the terminal shock. In the former case resulting distributions are very flat or even inverted ($\sigma < 3$, cf. Appendix B). This feature results from the character of the acceleration process with particles having an opportunity

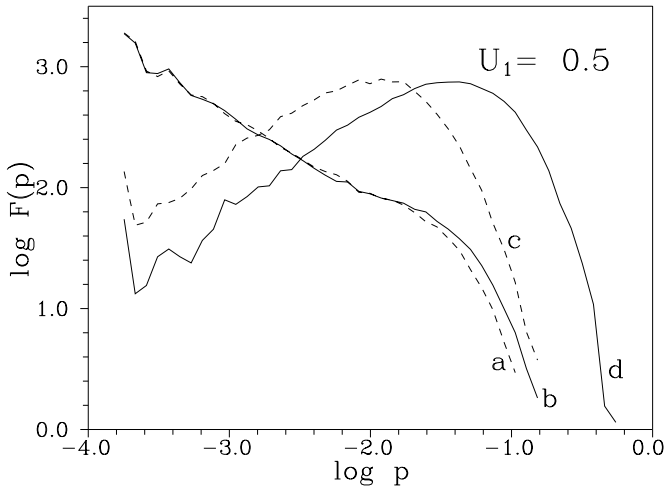

Fig. 6. Comparison of the particle spectra formed with wide ($R_{esc} = 11.0$; dashed lines (a) and (c)) and narrow ($R_{esc} = 2.0$; full lines (b) and (d)) cocoon. The results are presented for $L_{esc} = 1.0$ and two possibilities for particle injection: $z_{inj} = 0.0$ for cases (a) and (b), and $z_{inj} = -1000.0$ for the cases (c) and (d).

to hit the accelerating surface again and again due to an inefficient diffusive escape to the sides. The apparent deficiency of low-energy particles in these spectra results from the fact that most of these particles succeeded in crossing the discontinuity several times before they are able to diffusively escape through the side boundary. In other words, the escape due to particle energy increase (and the corresponding diffusion coefficient increase) is much more effective than the escape caused by diffusion of the low energy particles across the cocoon. If we neglect the tangential discontinuity acceleration, the particle advection toward the terminal shock appended with the side boundary diffusive escape determines an initial phase of the upstream transport. The final energy spectrum is formed at the shock.

We also performed simulations with the continuous injection process extended along the jet boundary from $z = -1000$ up to the shock at $z = 0$. As long as most particles were injected far from the shock the resulting spectra were very similar to the ones obtained with $z_{inj} = -1000$.

The role of the cocoon spatial extension in the acceleration process can be evaluated from Fig-s 4,6. One may note that for the particle injection at the terminal shock in the presence of a nearby front boundary, any change in R_{esc} is accompanied by only a minor modification to the spectrum seen at highest energies. This behaviour is determined by the efficient particle escape through the front boundary. Only increasing L_{esc} to values $\gg L_{diff}(p = p_0)$ allows the larger R_{esc} to increase the spectrum cut-off substantially. However, for the injection far upstream of the shock the main process removing particles from the acceleration is the diffusive escape through the side boundary. In such a case particles can reach larger energies with a more extended cocoon. For the shock injection, the spectra presented in Fig. 6 only insignificantly differ in the momentum range between 10^{-4} and 10^{-2}. This feature illustrates the fact that spectrum inclination depends on the local conditions near the shock if the particle energy is insufficient to allow for non-diffusive escape through the boundary. For the upstream injection the spectrum with smaller R_{esc} is shifted up in this momentum range because the larger proportion of all particles have a chance to escape at a given momentum. However, the spectrum inclination does not significantly depend on R_{esc} until a chance for particle escape becomes comparable to the probability of doubling its energy. The process can be described in the following way. After commencing the acceleration process at injection, the energized particles fill diffusively the volume near R_j. The normal to the jet boundary diffusion coefficient is proportional to particle momentum in our model. Thus the diffusing relativistic particles fill this volume in a time inversely proportional to the particle momentum, $\propto p^{-1}$, and the time required for these particles to diffuse back to the jet boundary to be further accelerated is also $\propto p^{-1}$. As energy gains of particles interacting with the jet boundary - with the mean value depending on the particle anisotropy and the jet velocity - are proportional to p, the resulting spectrum inclination only slightly depends on the size R_{esc} at energies much smaller than the cut-off energy. A simplified analytic approach to this acceleration process is presented in Appendix B.

In Fig. 7, the spectra for different turbulence levels defined by the respective values of $D = 0.97$ or 0.0013 are compared. Because in the simulations with smaller D, particles were injected at larger initial momentum, in order to make the comparison more simple, we scaled (i.e. vertically shifted) the spectrum (a) to coincide in the power-law section with the spectrum (b). One can observe that the cross-field diffusion, changing as $\approx D^{1/2}$, has a substantial influence on the spectrum if the particle radial diffusion is the main process removing particles from the jet vicinity.

4. Final remarks

Application of the 'pure' shock acceleration mechanism in order to model UHE particle production in the discussed extragalactic jets meets a number of difficulties. Due to small spatial dimensions of hot spot regions, the diffusive particle escape may become a serious problem for particles, preventing them from reaching energies above 10^{20} eV. We would like to note that the respective losses would be enhanced in the presence of oblique fields causing the drift motions along the shock surface. Therefore it is not clear if the speeding up of the acceleration process at oblique shocks will be accompanied by the spectrum cut-off energy increase. In the super-luminal magnetic field configuration, the acceleration to UHE can be completely suppressed if there is no other mechanism providing particles in the sub-UHE energy range (cf. Begelman & Kirk 1990, Ostrowski 1993a). Another difficulty may arise due to the high inclination of the spectrum, $\sigma > 4.0$, expected in some cases in relativistic shocks (Ostrowski 1991, 1993a; Ballard & Heavens 1993). In realistic conditions it can substantially increase the shock wave energy conversion into lower energy cosmic rays. The total efficiency

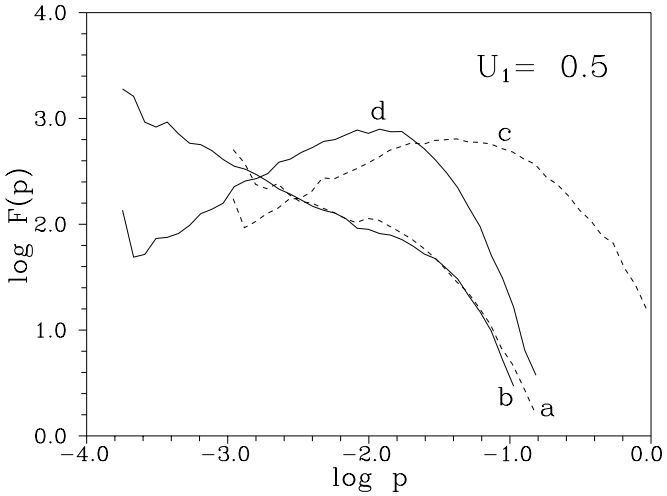

Fig. 7. Particle spectra formed with $D = 0.97$ (full lines; $p_0 = 1.8\,10^{-4}$) versus the spectra for the small $D = 0.0013$ (dashed lines; $p_0 = 10^{-3}$). The spectra (a) and (b) are formed for the shock injection $z_{inj} = 0$, while the spectra (c) and (d) for the jet boundary injection at $z_{inj} = -1000.0$. All presented results were derived with $R_{esc} = 2.0$ and $L_{esc} = 1.0$.

of cosmic ray generation must then be much larger to allow for the required power in UHE particles.

The presented hypothesis for the acceleration mechanism producing the most energetic cosmic ray particles at the jet side-boundary has a number of advantages over the 'pure' shock hypothesis. At first, its efficient action is rather weakly dependent on detailed conditions in the acceleration site. The mean magnetic field elongated along the jet axis assumed in the present paper is in no way essential to the presented discussion. One may note, however, that such a field configuration can be produced in a natural way due to any form of viscosity near the jet boundary, including the viscous pull of magnetized plasma mediated by the accelerated particles (Eq. 2, cf. Paper I). Then, the field perturbations required near the boundary are created by growing short wave instabilities at the jet boundary surface, as well as by the anisotropically distributed cosmic rays streaming along the boundary. The required energy expense of the jet for the UHE cosmic ray production is quite reasonable in comparison to the energy available. Within the present model involving relativistic jets, as long as global instabilities do not disrupt the organized jet flow, the cut-off energy can be a factor of a few ones greater than the value obtained in the pure shock acceleration if seed particles for acceleration are injected all the way along the jet boundary. Then, the obtained spectrum can be very flat before the cut-off. One may note that no compression or decompression is directly connected with this acceleration process and adiabatic losses seem not to be an obstacle here. A slow perpendicular expansion of the jet is in most cases controlled by the magnetic field structure and we do not expect it to play any noticeable role in particle deceleration within the UHE energy range. To recapitulate, we believe that because the respective conditions arise in a natural way, the process of particle acceleration at tangential discontinuity should be seriously considered as an important supplementary process to shock acceleration.

The main difficulty in analysing the details of the particle spectrum comes from an inadequate knowledge of local conditions in the acceleration region inside the jet and in the space surrounding the jet, including the magnetic field strength and configuration, the form and the amplitude of field perturbations, the distance of the 'effective' escape boundary or, finally, at low particle energies, the velocity profile of the turbulent shear layer expected to occur at the interface between the jet and the surrounding medium. Of course, observations provide some information about magnetic field magnitude and the mean field structure, but, besides its fragmentary, projection and resolution dependent character, the measurements relate to regions where radiative losses of cosmic ray electrons take place, not necessarily strictly coinciding with the ion acceleration sites. The information to be borrowed from hydrodynamical jet simulations usually refers to the flows with limited values of the magnetic field (cf. Marti et al. 1995, 1997; Gómez et al. 1995). So, the available basic information required for the cosmic ray spectrum derivation is very limited. Fortunately, the rapid acceleration at the velocity discontinuity results in very flat spectra in all situations where particles near the discontinuity have a chance to cross this surface at least few times before the escape. When considering the energy budget of accelerated particles, the flat spectrum means that cosmic ray energy is contained in particles with highest energies. In the conditions of effective acceleration, the upper scale for the UHE particle energy density is provided by the magnetic field energy density near the jet boundary. Possessing the higher energy density, UHE cosmic rays would smear out the discontinuity into a wide shear layer with a much reduced acceleration efficiency.

Finally, let us comment on the particle spectrum in the presence of radiative loses decreasing the cut-off energy in the spectrum. If the loss process can be sufficiently effective to shift the cut-off energy substantially below the 'geometric' cut-off present in our simulations, there will occur weaker mixing of the two acceleration processes in forming the total spectrum. No mixing means that there are two acceleration time scales present, the one for the shock acceleration and the other one for the tangential discontinuity acceleration. The spectra formed in these two processes – at the shock and at the jet boundary far from the shock – can be independent, with a different shape and an energy cut-off. For electrons the radiative cut-off can occur at such low energies that the acceleration process at the jet boundary involves only other processes (e.g. the second-order Fermi acceleration, highly oblique shocks, magnetic field reconnection) in the turbulent boundary layer, with the viscous shear acceleration playing only a secondary role (cf. Ostrowski 1997). Without a detailed consideration it is difficult to draw any conclusions about the resulting synchrotron spectra. We would like to note, however, that some observations of the synchrotron optical jets may require such mechanisms to operate (Ostrowski, in preparation). Till now the most detailed information available about the synchrotron jet structure is for the nearby M87 jet (e.g. Sparks et al. 1996, and references therein), but at least five more

have been observed. However, the observations are not conclusive in the matter of the particular mechanism responsible for the energetic particle populations present in these sources.

Acknowledgements. The present work was supported through the grants PB 1117/P3/94/06 and PB 179/P03/96/11 from the *Komitet Badań Naukowych*.

Appendix A: modelling of the particle acceleration process

We consider the particle diffusion in the jet-cocoon region in the case of the mean magnetic field being parallel to the jet velocity both inside and outside the jet. Modelling of the diffusive particle trajectories is based on the small-amplitude pitch-angle scattering approach (Ostrowski 1991). It assumes that the particle diffusion coefficients parallel to the mean field, $\kappa_{\parallel}$, and the one perpendicular to the mean field, $\kappa_{\perp}$, are proportional to the particle momentum. Due to this fact, the amount of computations required for reproducing particle diffusive trajectories for low energy particles is much larger than the respective amount for particles with higher energies. Therefore, in order to deal with these low energy particles, we introduced a hybrid approach to derive particle trajectories. For particles near the surfaces of the flow velocity change at the jet boundary and at the shock, and not further than 2 particle gyroradii away in the former case and 1 diffusive scale $\kappa_{\parallel,i}/U_i$ ($i = 1, 2$) from the shock surface, we use the exact form of the mentioned pitch-angle scattering method. When the particle diffuses further away from the respective discontinuity, we use the spatial diffusion model involving large time steps. However, the step length is always limited in order to prevent particles from crossing any discontinuity in an individual 'diffusive' step - the mean diffusive step allows only for moving a particle 0.25 of the distance to its closest boundary. In these computations we use the values of $\kappa_{\parallel}$ and $\kappa_{\perp}$ derived in independent simulations involving the 'exact' pitch-angle diffusion procedure. This way we are able to consider particles with momenta which differ in a few orders of magnitude. During the simulations we use a variant of the trajectory splitting procedure described by Ostrowski (1991). A good test for this simulation procedure is provided by the agreement of our shock accelerated spectra fitted at low energies with the values derived analytically by Heavens & Drury (1988).

Appendix B: on the spectrum of particles accelerated at the tangential discontinuity

Let us consider a simple model for particles accelerated at the plane tangential discontinuity surrounded with infinite regions for particle diffusion. We derive the stationary spectrum at the discontinuity for the perpendicular (to discontinuity) diffusion coefficient being proportional to particle energy, $\kappa_{\perp} \propto E$. For relativistic particles with $p = E$ and the same velocity $v = c$, the mean time between the successive particle interactions with the discontinuity is also proportional to the particle's energy. Thus the mean rate of particle energy gain is constant, independent of energy, $< \dot{p} >$ = const. The transport equation for the *phase-space* distribution function $f(p)$ has the following form,

$$\frac{1}{p^2}\frac{\partial}{\partial p}\left[p^2 < \dot{p} > f(p)\right] = Q_0\delta(p - p_0) \qquad . \qquad (B1)$$

In the above equation one assumes a continuous particle injection at $p = p_0$. For a general power-law form for $< \dot{p} >= C_0 p^{\alpha}$ it yields the solution,

$$f(p) = \frac{Q_0 p_0^2}{C_0}\, p^{-2-\alpha}\, H(p - p_0) \qquad , \qquad (B2)$$

where $H(x)$ is the Heaviside step function. As long as there are no specific energy scales introduced into the acceleration process the obtained form for $f(p)$ is independent of the velocity difference at the discontinuity (particle anisotropy), and of possible correlation between the interaction time and the energy gain. In the case considered in the present paper $\alpha = 0$ and $f(p) \propto p^{-2}$.

For the discontinuity formed at the jet boundary, the jet radius and the escape boundary radius provide energy scales to the process. As a result, a cut-off occurs at large energies in the spectrum. However, at small energies, where the jet boundary curvature is insignificant and the diffusive regions very extended, the solution should be close to the one given in (B2). In fact, numerical fits for low energy sections of cases (c) and (d) at Fig. 6 give the respective fits $f(p) \propto p^{-2.16}$ and $\propto p^{-2.10}$ (the difference in the obtained spectral indices is not significant, depending on the momentum range used for fitting).

References

Ballard K.R., Heavens A.F., 1991, MNRAS, 251, 438
Ballard K.R., Heavens A.F., 1992, MNRAS, 259, 89
Begelman M.C., Kirk J.G., 1990, ApJ, 353, 66
Bednarz J., Ostrowski M., 1996, MNRAS, 283, 447
Berezhko E.G., 1990, Preprint *Frictional Acceleration of Cosmic Rays*, The Yakut Scientific Centre, Yakutsk
Biermann P.L., 1994, Lecture at the Chinese Academy of Sciences - Max Planck Society Joint Seminar, Nandaihe, China (MPIfR preprint)
Biermann P.L., Rachen J.P., Stanev T., 1995, in Proc. 24th Int. Cosmic Ray Conf., Rome
Bridle A.H., Hough D.H., Lonsdale C.J., Burns J.O., Laing R.A., 1994, AJ, 108, 766
Celotti A., Fabian A.C., 1993, MNRAS, 264, 228
Coleman C.S., Bicknell G.V., 1988, MNRAS, 230, 497
Earl J.A., Jokipii J.R., Morfill G., 1988, ApJ, 331, L91
Elbert J.W., Sommers P., 1995, ApJ, 441, 151
Ellison D.C., Jones F.C., Reynolds S.P., 1990, ApJ, 360, 702
Fedorenko V.N., Courvoisier T.J.-L., 1996, A&A, 307, 347
Geddes J., Quinn C., Wald R.M., 1996, ApJ, 459, 384
Ghisellini G., Padovani P., Celotti A., Maraschi L., 1996, ApJ, 407, 65
Gómez J.L., Marti J.M[a], Marscher A.P., Ibáñez J.M[a], Marcaide J.M., 1995, ApJ, 449, L19
Hayashida et al., 1996, Phys. Rev. Lett., 77, 1000
Heavens A., Drury L'O.C., 1988, MNRAS, 235, 997
Henriksen R.N., 1987, ApJ, 314, 33
Jokipii J.R., Kota J., Morfill G., 1989, ApJ, 345, L67

Kang H., Ryu D., Jones T.W., 1996, ApJ, 456, 422
Kang H., Rachen J.P., Biermann P.L., 1997, MNRAS, 286, 257
Kirk J.G., 1997, in *Relativistic Jets in AGNs*, eds. M. Ostrowski, M. Sikora, G. Madejski, M. Begelman (Cracow)
Kirk J.G., Heavens A., 1989, MNRAS, 239, 995
Kirk J.G., Schneider P., 1987, ApJ, 315, 425
Kirk J.G., Schneider P., 1988, A&A, 201, 177
Marti J.M^{a}, Müller E., Font J.A., Ibáñez J.M^{a}, 1995, ApJ, 448, L105
Marti J.M^{a}, Müller E., Font J.A., Ibáñez J.M^{a}, Marquina A., 1997, ApJ, 479, 151
Medina Tanco G.A., 1998, ApJL (in press).
Medina Tanco G.A., de Gouveia Dal Pino E.M., Horvath J.E., 1997, Astropart. Phys., 6, 337
Meisenheimer K., Röser H.-J., Hiltner P.R., Yates M.G., Longair M.S., Chini R., Perley R.A., 1989, A&A, 219, 63
Naito T., Takahara F., 1995, MNRAS, 275, 1077
Newman P.L., Moussas X., Quenby J.J., Valdes-Galicia J.F., Theodossiou-Ekaterinidi Z., 1992, A&A, 255, 443
Ostrowski M., 1990, A&A, 238, 435 (Paper I)
Ostrowski M., 1991, MNRAS, 249 , 551
Ostrowski M., 1993a, MNRAS, 264, 248
Ostrowski M., 1993b, in Proc. 23rd Int. Cosmic Ray Conf., p. 329 (OG 9.3.6) Calgary
Ostrowski M., 1994, Comments on Astrophys., 17, 207
Ostrowski M., 1996, in Proc. ICRR Symp. on *Highest Energy Cosmic Rays*, ed. M. Nagano, Tanashi (p. 377)
Ostrowski M., 1997, in *Relativistic Jets in AGNs*, eds. M. Ostrowski, M. Sikora, G. Madejski, M. Begelman (Cracow)
Ostrowski M., Schlickeiser R., 1996, Solar Phys., 167, 381
Rachen J.P., Biermann P., 1993, A&A, 272, 161
Rachen J.P., Stanev T., Biermann P., 1993, A&A, 273, 377
Sigl G., 1996, Space Sci. Rev., 75, 375
Sigl G., Schramm D.N., Bhattacharjee P., 1995, Astropart. Phys. 2, 401
Sigl G., Schramm D.N., Lee S., Coppi P., Hill Ch.T., 1997, Proc. Natl. Acad. Sci. USA, Vol. 94, 10501
Sparks W.B., Biretta J.A., Macchetto F., 1996, ApJ, 473, 254
Stanev T., Biermann P.L., Lloyd-Evans J., Rachen J.P., Watson A.A., 1995, Phys. Rev. Lett., 75, 3056